

Assessment of factors influencing surface recrystallisation during high temperature exposure of fine-grained PM 2000 alloy

J.L. González-Carrasco^{a,*}, J. Chao^a, C. Capdevila^a, J.A. Jiménez^a,
V. Amigó^b, M.D. Salvador^b

^a Centro Nacional de Investigaciones Metalúrgicas (CENIM-CSIC), Avenida Gregorio del Amo no. 8, 28040 Madrid, Spain

^b Instituto de Tecnología de Materiales de la Universidad Politécnica de Valencia, Camino de Vera, s/n 46022 Valencia, Spain

Received 21 June 2006; received in revised form 1 March 2007; accepted 2 March 2007

Abstract

PM 2000 offers an excellent oxidation resistance that relies on its capability to develop in service a fine α -alumina scale, tightly adhered to the substrate. The advantages of the scale protection at low temperatures are obtained by performing a pre-oxidation treatment prior to operation. The aim of this study is to characterise the microstructural changes during oxidation (1100 °C/120 h) of the alloy in a fine-grained state, which make it more suitable for room temperature applications. With regards to the as-received material, oxidation treatment does not produce macroscopic changes in terms of grain size and texture. Beneath the scale, however, a shell about 10 μm thick containing coarse grains was formed. The grain size in this zone is in the order of the shell thickness, which is considerably higher than the grain size of about 2 μm for the remnant substrate. Microtexture analysis performed at these zones reveals that grains are oriented with the $\langle 111 \rangle$ and $\langle 110 \rangle$ direction parallel to the bar axis, which contrast with the weak $\langle 110 \rangle$ fiber texture of the bulk. The results presented in this work clearly confirm that surface recrystallisation is not related to oxidation-induced effects but to the heterogeneous deformation produced during grinding, that stimulate recrystallisation to occur at much lower temperatures.

© 2007 Elsevier B.V. All rights reserved.

Keywords: Recrystallisation; ODS alloys; Oxidation; Texture analysis

1. Introduction

The PM 2000 is an iron-base oxide dispersion strengthened (ODS) superalloy manufactured by a complex powder metallurgy route. As a first step, a mixture of metallic powders and dispersoids are mechanically alloyed to produce a final powder in which a fine dispersion of yttrium oxide particles is formed. The resulting powders are then canned and hot extruded and/or hot rolled. The microstructure at this stage presents submicron-sized elongated grains similar to that found in cold deformed materials [1]. A subsequent recrystallisation treatment at very high temperature (>1300 °C) yields a coarse microstructure with strongly elongated grains parallel to the extrusion direction, which is more suitable for high temperature applications.

Particularly attractive is the excellent oxidation resistance of the alloy that relies on the capability to develop a compact

and adherent α -Al₂O₃ scale at high temperature. During oxidation different transient alumina states can be formed, which are known to grow faster than α -alumina [2]. The transformation of metastable alumina phases into α -Al₂O₃ is an irreversible phenomenon that depends on exposure time and temperature, the metastable- α transition temperature being around 1000 °C [3]. Obviously, the higher the temperature the faster is the transformation process. If the alloy is to be used either at lower temperatures or under low-oxygen partial pressure environments, it has to be “pre-oxidised” at high temperature in pure oxygen or in air to develop the α -Al₂O₃ scale prior to operation.

Beneficial effects of a pre-oxidation treatment have been mainly found for coal gasification environments at intermediate temperatures [4–6] but this treatment can also be beneficial for other new applications at low temperatures. For example, it has been proposed that ferritic alloys could be promising candidates for surgical implants [7–9] because they combine the good mechanical properties of the metal substrate with the protective capacity of the alumina scale against physiological solutions [10]. The main limitation when using ferritic alloys

* Corresponding author. Tel.: +34 91 5538900; fax: +34 91 5347425.
E-mail address: jlg@cenim.csic.es (J.L. González-Carrasco).

at ambient temperature is that, like any BCC material, they exhibit a ductile–brittle transition (DBT) at around room temperature [11]. DBT temperature is related to the grain size, and in order to decrease this value a fine grain microstructure is required [12]. Therefore, to avoid the substrate recrystallisation the pre-oxidation temperature should be as low as possible. An optimum temperature for pre-oxidation of 1100 °C was selected since it yields a α -alumina scale with a few microns in thickness within reasonable production times. The analysis of the tensile and fatigue behaviour of pre-oxidised PM2000 [8] led to the conclusion that this treatment did not jeopardize the good mechanical properties of the fine-grained material. Moreover, toughness tests on pre-oxidised specimens indicated a significant increase of the impact energy [13], which is contrary to the embrittlement induced by the alumina scale in a similar pre-oxidised alloy [12,14–16]. As tensile and fatigue fractures can initiate at the scale–metal interface [8,12], this study is aimed at characterizing the microstructural changes during high temperature exposure, with special emphasis on the zones near the scale–metal interface. Since the texture could be of great importance for most mechanical properties [17], changes in the crystallographic orientation were investigated by using Electron Back Scattering Diffraction (EBSD) techniques.

2. Experimental part

The PM2000 alloy, nominally Fe–20Cr–5.5Al–0.5Ti–0.5Y2O3 (wt pct), was prepared at Plansee GmbH (Lechbruck, Germany) by mechanical alloying of a mixture of metallic powders and dispersoids, which were consolidated to obtain a hot rolled bar 35 mm in diameter. Microstructural investigations and texture analysis were performed on slices obtained from cylinders of 10 mm in diameter. The surface was abraded with silicon carbide papers, followed by polishing with diamond paste. In the final phase they were carefully polished with silica colloidal (40 nm). Specimens were finally washed in running water and then cleaned with alcohol.

Microstructural examination was performed by scanning electron microscopy (SEM) using a JEOL JSM 6500F microscope. Backscattered electron images (BEI) or Secondary Electron images (SEI) were obtained. Texture measurements in the as-received and annealed (1100 °C/120 h) conditions were performed in the back-reflected mode by X-ray diffraction using a X-ray diffractometer set-up with HI-STAR two dimensional multiwire proportional counter (General Area Detector Diffraction System, Bruker AXS). Co $K\alpha$ radiation was employed at a tube current of 30 mA and a voltage of 40 kV. The detector was cantered at $2\theta = 52.40^\circ$, 77.20° and 99.70° , with the centre of the detector 2θ position coupled with the beam incident angle θ . At each 2θ position enough planar frames were collected for covering the entire pole sphere. From the normalized and corrected X-ray data, the (1 1 0), (2 0 0) and (2 1 1) pole figures were reconstructed. The sample reference system was fiber, corresponding to the symmetry imposed by the hot rolling process. From these pole figures the orientation distribution function (ODF) was calculated, using the series expansion method ($l_{\max} = 22$) and ghost corrected. As ferrite present cubic symmetry, the orien-

tation density, $f(g)$, was represented in the reduced Euler space ($0 \leq \varphi_1, \Phi, \varphi_2 < \pi/2$). The samples for texture analysis were cut perpendicular to the longitudinal bar direction.

Microtexture analysis of pre-oxidised specimens was performed by EBSD at various locations on cross sections. The EBSD patterns were generated at an acceleration voltage of 20 kV and collected using a CRYSTAL detector of Oxford Instruments mounted in a SEM JEOL JSM6300. The indexing of the Kikuchi lines and the determination of the orientations were done with the software INCA developed by Oxford Instruments. The results were represented by means of an inverse pole figure (IPF) maps, which give the orientation of a macroscopic direction with respect to a specific crystal direction.

3. Results and discussion

Longitudinal and transverse sectioned samples of as-received bar revealed a fine-grained structure with a mean value of about 2 μm in diameter (Fig. 1). Although these grains appear slightly elongated along the longitudinal bar direction, the microstructure was homogeneous over the bar thickness. Texture analysis of the as-received material reveals a weak fiber texture characterized by the (1 1 0) direction parallel to the rolling axis. This texture is typical of BCC materials deformed by extrusion. During high temperature oxidation (1100 °C/120 h) a moderated grain growth occurs, which was macroscopically manifested by a small decrease in hardness and 0.2% yield strength [8]. No appreciable change in the texture from the starting condition was observed.

SEM examination of the oxidised sample revealed the presence of an alumina scale decorated with oxide nodules of a submicron size (Fig. 2a) although in a few cases they can reach 1 μm . Cross sectional examination reveals an even scale, the thickness of which ($\approx 4 \mu\text{m}$) is consistent with previous results on the oxidation kinetics for this alloy [9]. After etching, cross sectional views reveal that beneath the scale (Fig. 2b) a shell of coarse grains with an average size of about 10 μm is formed.

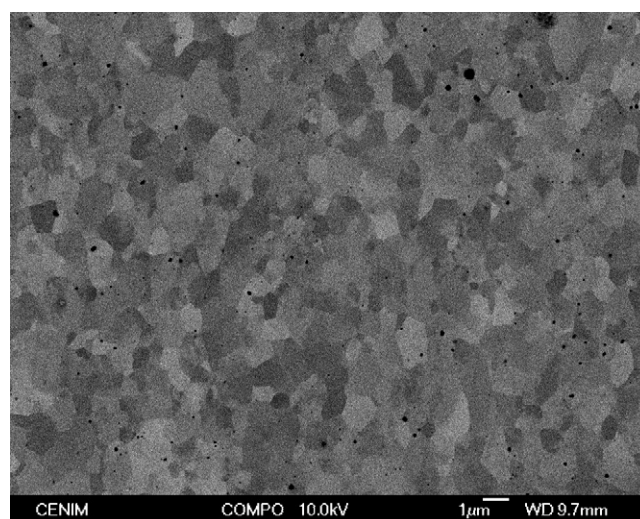


Fig. 1. BEI image of a cross sectional view of PM 2000 in the as-received condition that highlights the different crystallographic contrast of grains.

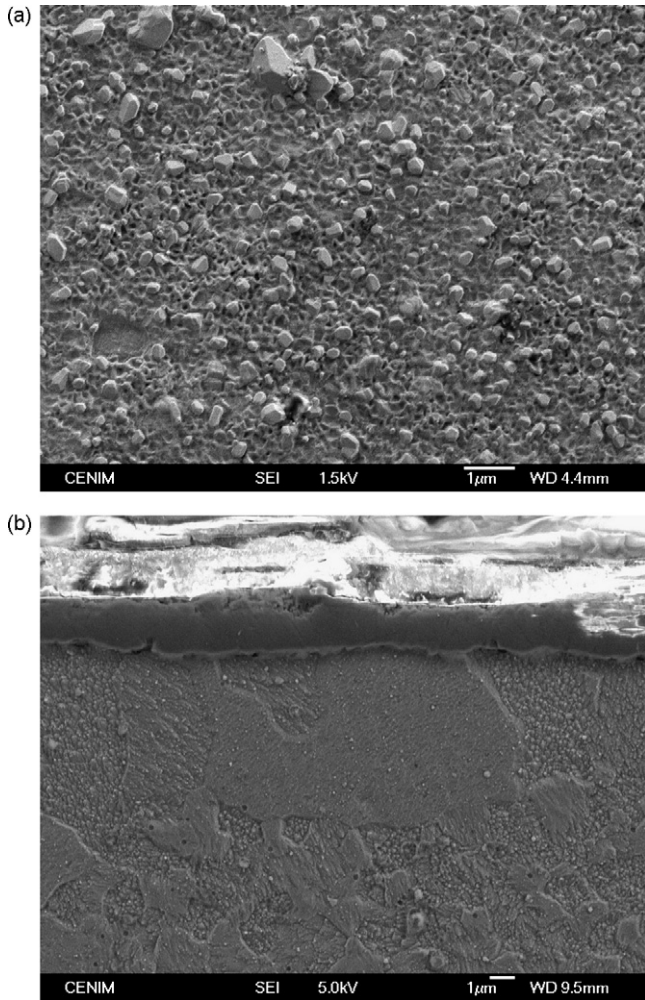


Fig. 2. (a) Oxide nodules decorating the outer part of the alumina layer obtained during pre-oxidation heat treatment. (b) Shell of coarser grains in the interface between alumina scale and the matrix revealed by etching of the specimen.

Occasionally, the coarse grained zone can be wider and a maximum width of about 500 µm was measured. A local grain growth beneath the alumina scale has been also reported for the intermetallic ODS alloy Fe40AlGrade 3 [18].

For a deeper understanding of the microstructural changes beneath the scale a microtexture analysis was performed. Fig. 3 shows an orientation map of an area near the surface. The correspondence between the contrast of the different grains and the crystallographic orientation is indicated in the stereographic triangle. This figure reveals that the population of grains with a $\langle 111 \rangle$ orientation is higher near the surface (area between dashed lines) and decreases towards the centre of the sample. Likewise, the misorientation of grain boundaries was measured. Fig. 4 shows a normalised distribution of misorientation angles obtained from a single orientation measurements made by EBSD. It can be observed that the population of high angle boundaries is high. This result, along with the absence of a subgrain structure, allows us to conclude that oxidation at this temperature yields beneath the scale not only to a local grain growth but also to a change in the grain orientation. Both results seem to confirm that a true recrystallisation

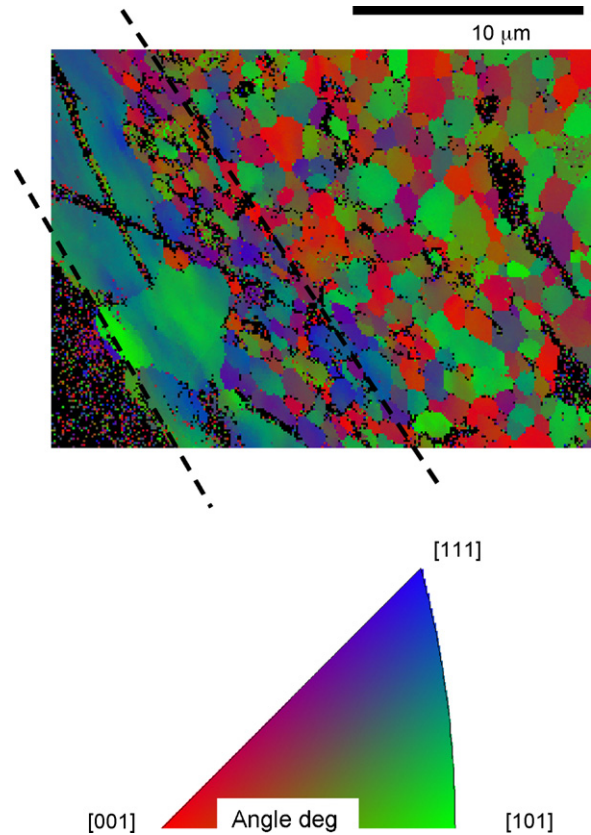


Fig. 3. EBSD image of recrystallised grains near to the scale–matrix interface.

sation process took place in this zone during the preoxidation treatment.

Recrystallisation of ODS alloys mostly occurs at exceptionally high homologous temperatures, in this alloy about $0.9T_m$, where T_m is the melting temperature (1487 °C). Thus, the most important question that arose in this investigation is why the recrystallisation temperature drops near the scale–matrix interface. Taking into consideration that crystallographic orientation of grains agrees with the texture of this alloy after recrystallisation at higher homologous temperatures [19], a similar

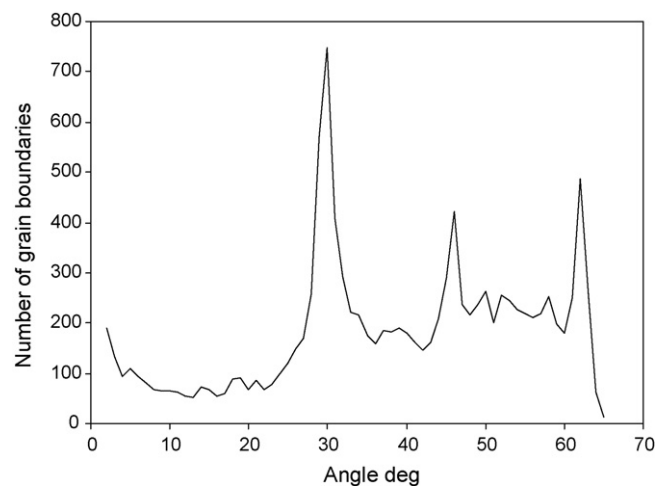


Fig. 4. Normalised distributions of misorientation obtained by EBSD.

recrystallisation mechanism can be assumed. According to this mechanism, the boundary junctions of small grains act themselves as severe pinning lines, which lead to an enormous activation energy for the nucleation of recrystallisation [20]. This activation energy is reduced if a few grains are larger; indeed, any non-uniformity introduced into the microstructure, for example by inhomogeneous deformation, will lead to a large decrease in the recrystallisation temperature [21,22].

With regards to the role of the oxidation process on the surface recrystallisation, it could be argued that inwards alumina scale growth during high temperature oxidation [2] causes a volume increase at the scale–metal interface, yielding to a local plastic deformation of the substrate. The phenomenon is easily revealed by the presence of imprints beneath the scale, clearly visible at places where detachment of the scale has occurred [12]. In order to clarify if this recrystallisation process is related with the deformation induced by the growth of the oxide layer, a set of specimens with three different surface conditions were pre-oxidised at 1100 °C, namely: as-ground, as-ground plus polished, and as-polished plus acid etching (10 ml acetic acid, 10 ml HNO₃, 15 ml of HCl and 3 drops of glycol). The as-ground condition is expected to retain a thin layer of heavily deformed

material whereas polished and etched surfaces should hardly show any microstructural change. A close sectional examination by SEM of oxidised specimens revealed that only the ground and oxidised surface contains a subscale layer of larger grains (Fig. 5). This clearly confirms that the recrystallisation of oxidised samples is not related to oxidation-induced effects but to the heterogeneous deformation produced during machining, stimulating recrystallisation to occur at much lower temperatures [23].

Cold deformation was found to account for the modification of local crystallographic texture [24]. The importance of this texture change beneath the surface on triggering recrystallisation is two fold. Firstly, for reasons which are not obvious, recrystallisation seems easiest whenever the $\{111\}\langle\bar{1}10\rangle$ is prominent [25], which is consistent with the microtexture measurements shown in Fig. 3. Secondly, the texture could lead to the clustering of adjacent grains into similar orientations. This would lead to an increase in the effective grain size, thereby making the nucleation of recrystallisation easier [21].

Mechanical properties at room temperature of ODS alloys are known to be strongly sensitive to texture of the material. Therefore, recrystallisation beneath the scale during high temperature exposure may play a critical role when considering applications where fatigue strength, dominated by the surface microstructure, is sought. This feature will obviously be more relevant for the mechanical behaviour of very thin components.

4. Conclusions

This paper analyses the microstructural changes produced in the vicinity of the α -Al₂O₃ scale–matrix interface during the pre-oxidation treatment. It can be concluded that the shell of recrystallised grains formed at the α -Al₂O₃ scale–matrix interface of oxidised samples is not related to oxidation-induced effects but to the heterogeneous deformation produced during machining. This result provides additional evidence about how strain heterogeneities in the microstructure promote the nucleation of recrystallisation, stimulating recrystallisation to occur at a much lower temperature.

On the other hand, EBSD study of the crystallographic orientations of both the recrystallised grains themselves and the unrecrystallised grains in their vicinity shows that deformation during machining induces a $\{111\}$ texture that, as several authors have reported, enhances nucleation of recrystallisation.

Acknowledgements

The authors thank financial support to CICYT (Spain) under Project ENE2006-15170-C02-01/ALT.

References

- [1] E.A. Little, D.J. Mazey, W. Hanks, *Scr. Metall. Mater.* 25 (1991) 1115–1118.
- [2] K.M.N. Prasanna, A.S. Khanna, W.J. Ramesh Chandra, *Quadakkers, Oxid. Met.* 46 (5/6) (1996) 465–480.
- [3] J. Doychak, M. Rühle, *Oxid. Met.* 31 (1989) 431–452.

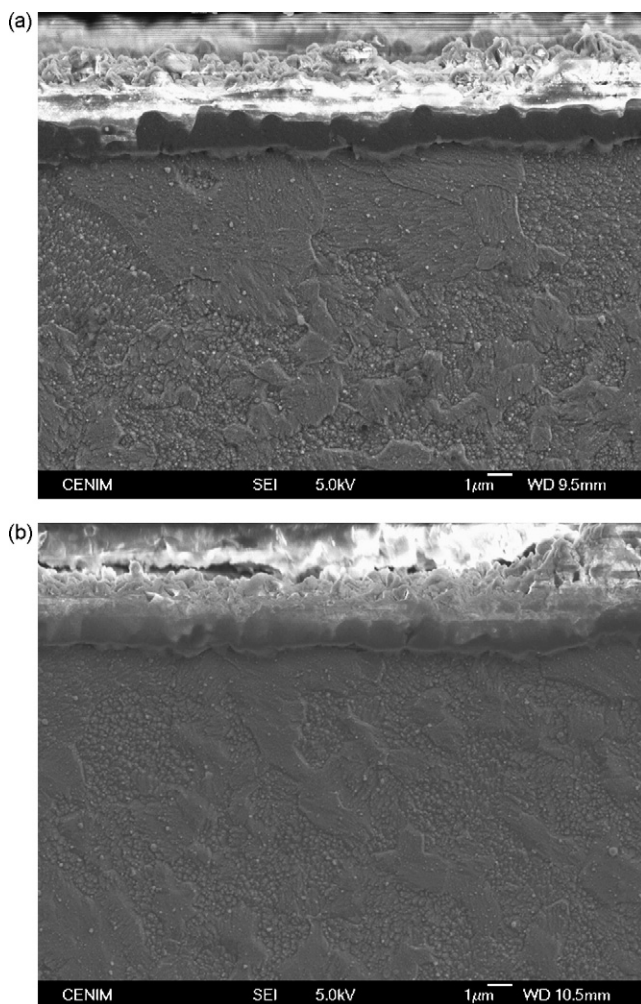


Fig. 5. SEI images of specimens oxidised at 1100 °C/120 h after: (a) grinding and (b) polishing/acid etching.

- [4] V. Guttman, A. Mediavilla, O. Ruano, *Mater. High Temp.* 11 (1993) 42–50.
- [5] M. Lloyd, *Proc. Frontiers of High Temperature Materials II*, London, 1983, pp. 419–441.
- [6] P.S. Sidky, M.G. Hocking, *Corros. Sci.* 29 (1989) 735–765.
- [7] M.L. Escudero, J.L. González-Carrasco, *Biomaterials* 15 (1994) 1175–1180.
- [8] J.L. González-Carrasco, G. Ciapetti, M.A. Montealegre, S. Pagani, J. Chao, N. Baldini, *Biomaterials* 26 (2005) 3861–3871.
- [9] G. Strehl, J.L. González-Carrasco, J.L. Peris, M.A. Montealegre, S. García, C. Atienza, G. Borchardt, *Surf. Coat. Technol.* 201 (1–2) (2006) 148–156.
- [10] J.L. González-Carrasco, M.C. García-Alonso, M.A. Montealegre, M.L. Escudero, J. Chao, *Oxid. Met.* 55 (2001) 209–221.
- [11] J.M. Davidson, in: J.S. Benjamin, R.C. Been (Eds.), *Frontiers of High Temperature Materials II*, IncoMAP, London, 1983, p. 163.
- [12] J. Chao, J.L. González-Carrasco, J. Ibañez, M.L. Escudero, G. González-Doncel, *Metall. Mater. Trans.* 27A (1996) 3809–3816.
- [13] J. Chao, unpublished results.
- [14] J.M. Davidson, *Proc. Frontiers of High Temperature Materials II*, London, 1983, pp. 163–189.
- [15] T. Hughes, T. Hirst, *Proc. Frontiers of High Temperature Materials II*, London, 1983, pp. 149–162.
- [16] J.M. Davidson, C.M. Austin, M.L. Robinson, *Metall. Trans.* 14A (1983) 1516–1518.
- [17] J. Chao, M.C. Cristina, J.L. González-Carrasco, G. González-Doncel, in: L. Lecomte-Beckers, F. Schubert, P.J. Ennis (Eds.), *Proc. Conf. “Materials for Advanced Power Engineering 1998” Part II*, Forschungszentrum Jülich GmbH, 1998, p. 827.
- [18] J. Chao, D.G. Morris, M.A. Muñoz Morris, J.L. González-Carrasco, *Intermetallics* 9 (2001) 299–308.
- [19] C. Capdevila, Y.L. Chen, N.C.K. Lassen, H.K.D.H. Bhadeshia, A.R. Jones, *Mater. Sci. Tech. Ser.* 17 (2001) 693–699.
- [20] W. Sha, H.K.D.H. Bhadeshia, *Mater. Sci. Eng. A* 223 (1997) 91–98.
- [21] C. Capdevila, U. Miller, H. Jelenak, H.K.D.H. Bhadeshia, *Mater. Sci. Eng. A* 316 (2001) 161–165.
- [22] C. Capdevila, Y.L. Chen, A.R. Jones, H.K.D.H. Bhadeshia, in: N. Hansen, X. Huang, D. Juul Jensen, E.M. Lauridsen, T. Leffers, W. Pantleon, T.J. Sabin, J.A. Wert (Eds.), *Proc. of the 21st Riso International Symposium on Materials Science*, Riso National Laboratory, Denmark, 2000, p. 277.
- [23] C. Capdevila, Y.L. Chen, N.C.K. Lassen, H.K.D.H. Bhadeshia, A.R. Jones, *Mater. Sci. Technol.* 17 (2001) 693–699.
- [24] T.S. Chou, H.K.D.H. Bhadeshia, *Mater. Sci. Technol.* 9 (1993) 890–897.
- [25] C. Capdevila, H.K.D.H. Bhadeshia, *Adv. Eng. Mater.* 3 (2001) 647–656.